

Out-of-Plane Modes of *cis*-1,3,5-Hexatriene: Frequency Shifts in the 2^1A_1 and 1^1B_1 Excited States[†]

Clemens Woywod*, James A. Snyder, and John H. Frederick[‡]

Department of Chemistry and Program in Chemical Physics, University of Nevada, Reno, Nevada 89557-0020

Received: October 17, 2000; In Final Form: January 28, 2001

The calculation of Hessian matrices for the out-of-plane modes of *cis*-1,3,5-hexatriene (CHT) in the 1^1A_1 , 2^1A_1 , and 1^1B_1 states is reported at the equilibrium geometry of the electronic ground state. The complete-active-space self-consistent-field (CASSCF) electronic structure model is employed. π and σ orbitals are included in the active space to account for the mixing of both types of molecular orbitals at nonplanar conformations of CHT. On the basis of the Hessian matrices and the resulting approximate normal frequencies, an interpretation of recent spectroscopic evidence for the valence excited states of CHT is attempted. In particular, we make assignments of transitions in the low-frequency region of the $h\nu + h\nu$ resonance enhanced multiphoton ionization (REMPI) spectrum of the 2^1A_1 state. The predicted excited-state frequencies appear to be accurate and normal coordinate rotations induced by electronic excitation are shown to play an important role for the intensity distributions observed by REMPI and resonance Raman spectroscopy.

I. Introduction

We have recently reported investigations^{1,2} of the vibronic coupling between the 2^1A_1 and 1^1B_1 states of *cis*-1,3,5-hexatriene (CHT) (the first singly excited $\pi \rightarrow \pi^*$ state is also frequently provided with the label “ 1^1B_2 ”; for brief discussions of this issue, see Refs 1 and 3. Only modes of a_1 and b_1 symmetry are able to couple in first order to the $1^1A_1 \rightarrow 2^1A_1$ and $1^1A_1 \rightarrow 1^1B_1$ transitions if vibronic interactions with other electronic states are not exactly included in the Hamiltonian for the nuclear motion. The characterization of the potential energy surfaces and the dynamical calculations in Refs 1 and 2 have therefore been restricted to subspaces spanned by normal coordinates transforming according to these two irreducible representations of the C_{2v} point group.

The resonance Raman (RR) emission of the 2^1A_1 ^{5,6} and 1^1B_1 ^{5,6} states of vapor phase CHT, as well as information obtained by high-resolution techniques such as resonance enhanced multiphoton ionization (REMPI),^{7,8} fluorescence excitation⁹ and direct absorption spectroscopy^{10,11} of both states in free jet expansions, indicate, however, that out-of-plane displacements contribute to the respective intensity distributions. This is particularly true of the low-frequency portion of the $h\nu + h\nu$ REMPI spectrum of the 2^1A_1 state^{7,8} and the enhancement of Raman profiles of torsional modes for excitation energies on resonance with the 1^1B_1 state of CHT.^{5,6}

Many aspects of the involvement of out-of-plane distortions in the spectroscopy of the low-lying valence states of CHT are far from resolved.^{4,6–8} The model calculations presented in Refs 1 and 2 do not explicitly account for effects induced by vibrations of a_2 and b_2 symmetry and no excited-state force fields of high accuracy have been reported in the literature to support an interpretation of the spectroscopic results.

The observation that equilibrium geometries and Hessian matrices of high quality are not available for excited states even

of small molecular systems is quite general. One reason for this deficiency is that electronic structure methods based on a single configuration state function (CSF) are frequently not appropriate for the description of excited electronic states. Moreover, various problems can be encountered even if a multiconfigurational approach is attempted, for example, root flipping, adverse orbital rotations, or inadequate selection of configurations and symmetry breaking phenomena to name only a few. In a system like CHT, an obvious difficulty arises, for example, from the mixing of π - and σ -type orbitals if a calculation of ground and excited-state potential energies as a function of out-of-plane coordinates is considered, leading to a strong increase in the number of CSFs that need to be included in the configuration interaction (CI) expansion for a description of the valence states as compared to calculations at planar geometries.

Here, we address the problem of deriving the a_2 and b_2 symmetry blocks of the Hessian matrices for the 1^1A_1 , 2^1A_1 , and 1^1B_1 states of CHT at the ground-state equilibrium geometry by employing the complete-active-space self-consistent-field (CASSCF) electronic structure model^{12–16} with the main objectives of improving the analysis of spectra and of completing the parameter sets required for future model calculations of the excited-state dynamics of CHT.

II. Electronic Structure Methods

Kohler et al.⁸ and Olivucci et al.¹⁷ have carried out geometry optimizations and force field calculations for the 2^1A_1 state at the CASSCF level of theory, but frequency predictions have been published for two modes only (in Ref 17). Complete sets of normal frequencies in the 1^1B_1 state have been computed by Hemley et al.¹¹ with the semiempirical Pariser–Parr–Pople (PPP) Hamiltonian and by Zerbetto and Zgierski¹⁸ based on the single excitation configuration interaction (CIS) model. In Refs 8, 11, and 17, stable equilibrium geometries were obtained in C_{2v} symmetry for both excited states (Ref 8 reports two imaginary frequencies for the 2^1A_1 minimum at the CASSCF/STO-3G level of theory that disappear if a DZ basis set is used). CASSCF calculations performed by Rohlfing also find a bound C_{2v} structure in the 2^1A_1 state but the CASSCF and CIS methods

[†] Part of the special issue “William H. Miller Festschrift”.

* To whom correspondence should be addressed. E-mail: Clemens.Woywod@ch.tum.de.

[‡] E-mail: jhf@chem.unr.edu.

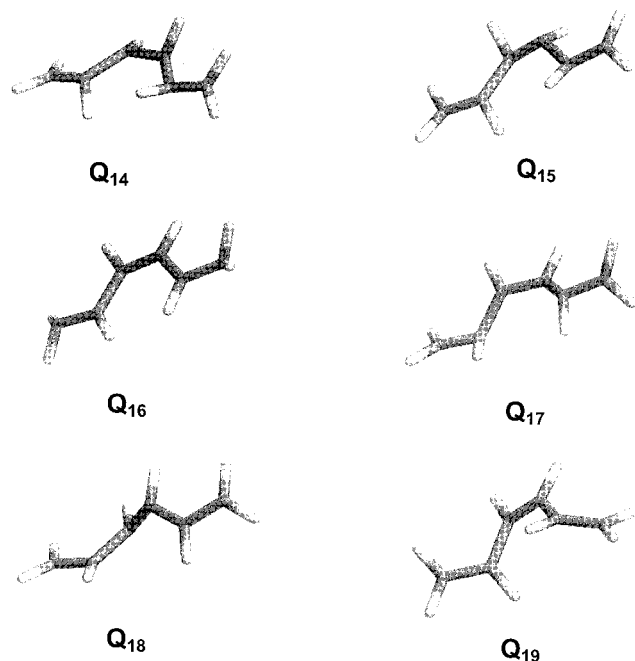
a_2 Modes

Figure 1. Displacements along the six a_2 symmetry ground-state normal coordinates of cis-1,3,5-hexatriene are shown. The geometries can be described by the C_2 point group.

predict a stabilization of the 1^1B_1 level for a rotation around the central C=C double bond similar to displacement along normal coordinate Q_{18} (see Figure 1), that is, a twisted minimum geometry of C_2 symmetry is postulated for the diabatically correlated 1^1B state.¹⁹ Ref. 18 also predicts saddle point character for the stationary point of the 1^1B_1 state in C_{2v} symmetry, but stabilization is expected to occur along the C–C single bond torsion coordinate Q_{19} (see Figure 1). The deviating CIS results of Refs 18 and 19 can probably be explained by the larger basis set (6-311++G(d,p) vs 6-31+G) employed by Rohlfing.

Geometry optimization and subsequent force field calculation represents an effective strategy for acquiring information about excited-state potential energy surfaces, but we pursue an alternative strategy in this work for the following reason: Second-order S_1 – S_2 coupling may contribute some intensity to combination bands of modes of a_2 and b_2 symmetry in the excitation spectra of the 2^1A_1 state in analogy to octatetraene,^{20,21} but we will concentrate in this study on second-order Franck–Condon activity as excitation mechanism for out-of-plane modes in the continuous wave (CW) absorption and RR spectra as well as in the free jet REMPI and fluorescence excitation spectra of the 2^1A_1 state of CHT. This is also true for the CW spectroscopy of the 1^1B_1 state. We assume that the intensities of vibrations of a_2 and b_2 symmetry in these spectra are largely determined by the curvature of the excitation energy functions of the 2^1A_1 and 1^1B_1 states at the ground state equilibrium geometry. The curvature of the potential energy as a function of nontotally symmetric displacements depends in general relatively weakly on small variations in the totally symmetric coordinates, but it is clear that an evaluation of the excited-state Hessian matrices at the ground-state minimum structure will yield more accurate on- and off-diagonal quadratic vibronic coupling constants for the out-of-plane modes than a calculation of the force fields at the 2^1A_1 and 1^1B_1 equilibrium geometries. The excited state frequencies, on the other hand, can be more accurately obtained

TABLE 1: Parameters $\gamma_{kl}^{(n)}$ for the Adiabatic 1^1A_1 (1^1A_{it} , $1^1A_{it}'$), 2^1A_1 (2^1A , $2^1A_{it}'$), and 1^1B_1 (1^1B , $1^1A_{it}''$) States of CHT, Calculated at the (5,5) CASSCF Level of Theory and Defined at The Equilibrium Geometry of the Electronic Ground State in Terms of S_0 Normal Coordinates^a

		a_2 -modes ($C_{2v} \rightarrow C_2$)					
state	mode	Q_{14}	Q_{15}	Q_{16}	Q_{17}	Q_{18}	Q_{19}
1^1A	Q_{14}	0.0640	-0.0008	-0.0012	-0.0012	-0.0003	0.0020
	Q_{15}		0.0592	0.0024	0.0010	-0.0005	-0.0003
	Q_{16}			0.0479	-0.0012	-0.0008	-0.0032
	Q_{17}				0.0418	0.0002	-0.0019
	Q_{18}					0.0198	0.0014
	Q_{19}						0.0107
2^1A	Q_{14}	0.0334	-0.0086	-0.0030	-0.0128	-0.0061	0.0147
	Q_{15}		0.0245	0.0030	-0.0132	0.0059	-0.0069
	Q_{16}			0.0095	0.0025	0.0029	-0.0017
	Q_{17}				0.0130	0.0000	-0.0074
	Q_{18}					0.0120	0.0059
	Q_{19}						0.0182
1^1B	Q_{14}	0.0591	0.0005	-0.0016	-0.0067	-0.0052	0.0151
	Q_{15}		0.0471	-0.0029	-0.0184	0.0067	-0.0051
	Q_{16}			0.0463	0.0009	0.0003	-0.0007
	Q_{17}				0.0285	0.0080	-0.0023
	Q_{18}					0.0115	0.0089
	Q_{19}						0.0039
		b_2 -modes ($C_{2v} \rightarrow C_s$)					
state	mode	Q_{32}	Q_{33}	Q_{34}	Q_{35}	Q_{36}	
$1^1A'$	Q_{32}	0.0676	0.0007	0.0014	-0.0002	-0.0005	
	Q_{33}		0.0473	-0.0010	0.0007	0.0008	
	Q_{34}			0.0491	0.0008	-0.0005	
	Q_{35}				0.0374	0.0002	
	Q_{36}					0.0070	
$2^1A'$	Q_{32}	0.0287	-0.0005	0.0004	0.0242	-0.0086	
	Q_{33}		0.0075	0.0046	-0.0043	-0.0002	
	Q_{34}			0.0345	0.0140	-0.0064	
	Q_{35}				0.0266	-0.0064	
	Q_{36}					0.0155	
$1^1A''$	Q_{32}	0.0606	-0.0001	-0.0021	0.0175	-0.0067	
	Q_{33}		0.0470	0.0044	-0.0029	0.0006	
	Q_{34}			0.0448	0.0079	-0.0066	
	Q_{35}				0.0327	-0.0003	
	Q_{36}					0.0081	

^a Units are eV.

from these force fields as opposed to the Hessian matrices obtained at the ground-state equilibrium structure.

We present here the complete Hessian matrices for the out-of-plane modes of CHT in the 1^1A_1 , 2^1A_1 , and 1^1B_1 states defined at the equilibrium configuration of the electronic ground state at the CASSCF level of theory (Table 1). The second derivatives of the potential energy functions are evaluated with respect to approximate ground-state normal coordinates derived from the MP2/aug-cc-pVDZ force field of the 1^1A_1 state (the MP2/aug-cc-pVDZ equilibrium geometry and harmonic frequencies of the 1^1A_1 state are discussed in Ref. 1). Cartesian geometries corresponding to finite displacements along linear combinations of internal symmetry coordinates that resemble ground state normal displacements as closely as possible were constructed based on the ab initio force field by an iterative procedure.¹

All electronic states considered in the present study are valence states^{1,3} and can be accurately represented by the moderately diffuse aug-cc-pVDZ basis set.²² However, a multiconfigurational approach is required for the description of the excited states. The covalent 2^1A_1 state is dominated by the doubly excited $(\pi_1)^2 (\pi_2)^2 (\pi_3)^0 (\pi_4)^2$ CSF but a large number of additional excitations within the valence space must be included to properly model the compact nature of the wave function in analogy to the correlated 2^1A_g state of THT.^{1,23,24} The singly excited $(\pi_1)^2 (\pi_2)^2 (\pi_3)^1 (\pi_4)^1$ CSF represents a good zeroth-order approximation to the 1^1B_1 wave function, but out-

out-of-plane distortions induce vibronic interactions with other configurations that make a multiconfigurational ansatz necessary also for this state and consideration of dynamic electron correlation effects has been shown to be essential to reproduce the valence character of the ionic 1^1B_1 wave function.^{1,3}

The six valence π orbitals constitute the appropriate active space for an accurate and consistent calculation of the 1^1A_1 , 2^1A_1 , and 1^1B_1 valence states of planar CHT employing the CASSCF method.¹ Because we are concerned with nonplanar geometries in this study, mixing of π and σ orbitals must further be taken into account in the selection of the active space, but the length of the CASSCF CI expansion increases rapidly with the number of active orbitals, imposing a limit of typically 12 orbitals on the maximum size of the active space.¹³ Moreover, the choice of the most important σ orbitals for an extension of the active space is not obvious. Linear combinations of π and σ orbitals occupying a similar energy range will generally exhibit a greater tendency to form molecular orbitals that need to be included into the active space upon out-of-plane distortion. However, the orbital energy criterion does not directly lead to an unambiguous identification of a sufficiently small subset of active σ orbitals for the electronic states under consideration. We have therefore investigated the addition of several combinations of σ orbitals to the valence π active space and found that inclusion of the two σ orbitals energetically enframing the π blocks in each of the two symmetry species characteristic of the C_2 and C_s point groups into the active space produces well-balanced results. Nonzero displacement along normal coordinates transforming according to the a_2 and b_2 irreducible representations reduces the symmetry of the nuclear frame of CHT from C_{2v} to C_2 and C_s (the symmetry plane being perpendicular to the molecular plane), respectively, and we will assign the label (5,5) to denote this active space in both point groups. This label refers to the number of active orbitals in the irreducible representations (A, B) and (A', A'') of the C_2 and C_s symmetry groups, respectively. Distributing 10 electrons over 10 orbitals defines the dimensions of the CASSCF calculations. The resulting CASSCF CI expansions comprise 9752 CSFs and 9652 CSFs for electronic states transforming according to the A (A') and B (A'') irreducible representations, respectively, of the C_2 (C_s) point group. The CASSCF calculations have been performed with the MOLCAS 4.0 package.²⁵

If the nuclear frame of CHT can be described by the C_2 (C_s) point group, we are primarily interested in the $1A$ ($1A'$), $2A$ ($2A'$), and $1B$ ($1A''$) states, which are diabatically correlated to the 1^1A_1 , 2^1A_1 , and 1^1B_1 states in C_{2v} symmetry. For the totally symmetric eigenvectors, an individual optimization scheme can be employed in the CASSCF calculations, but the convergence of the two lowest roots of B (A'') symmetry can be improved by including both in the CASSCF energy functional with equal weights. At the state-averaged CASSCF level of theory, the first root in the B (A'') representation is actually not identical to the first singly excited $\pi \rightarrow \pi^*$ state of CHT but to another low lying valence state of multiconfigurational character with significant contributions from doubly excited CSFs. This state has also been analyzed by Serrano-Andrés et al.³ and can be identified as the 2^1B_1 state within the C_{2v} point group. In the CASSCF calculations, we observe a strong dependence of the relative energetical ordering of both 1^1B_1 valence states on the specification of the active space and the optimization conditions, but the singly excited $\pi \rightarrow \pi^*$ state is correctly predicted as the 1^1B_1 state at the ground-state equilibrium geometry if dynamical electron correlation is included in the electronic

structure model via the single-state multiconfigurational second-order perturbation theory (CASPT2) method.²⁶

Difficulties are encountered, however, if CASPT2 calculations are performed at nonplanar geometries and no realistic frequencies could be obtained for the out-of-plane modes at this level of theory. The problems must be related to the mixing of π and σ orbitals in the wave function because accurate CASPT2 potential energy functions of all three states have been obtained for the in-plane vibrations of CHT in Ref 1. It is clear that the enlargement of the valence π active space by four σ orbitals cannot account for all CSFs that are relevant for a complete zeroth-order description of the low-lying valence states at nonplanar conformations of CHT, but inclusion of additional σ orbitals into the active space would lead to a prohibitive increase of the CASSCF CI expansion length.

The limitation of the active space to 10 orbitals only impairs the estimation of the dynamic correlation energy via CASPT2 but not the accuracy of the (5,5) CASSCF calculations, which yield a realistic description of the out-of-plane potential energy functions as will be seen from the discussion in the following section. The CASSCF approach generally overestimates vertical excitation energies, but this does not affect the computation of Hessian matrices for the excited states which represent the curvature of the potential energy surfaces. The 1^1B_1 wave function is too diffuse at the CASSCF level as mentioned above, but this does also not appear to significantly diminish the accuracy of the frequencies for this state.

The elements $\gamma_{kl}^{(n)}$ of the Hessian matrices γ presented in the next section are the coefficients of a second-order Taylor approximation of the adiabatic potential energy surfaces V_n of the 1^1A_1 , 2^1A_1 , and 1^1B_1 states of CHT around the S_0 equilibrium geometry in terms of dimensionless ground-state normal coordinates Q_k according to

$$V_n(Q_k, Q_l) \approx E_n + \sum_{kl} \gamma_{kl}^{(n)} Q_k Q_l \quad (2.1)$$

E_n denotes the vertical excitation energy of electronic state $|\phi_n\rangle$, and the $\gamma_{kl}^{(n)}$ are formulated according to

$$\gamma_{kl}^{(n)} = \frac{1}{2} \left\langle \phi_n \left| \frac{\partial^2 \hat{H}_{el}}{\partial Q_k \partial Q_l} \right| \phi_n \right\rangle \quad (2.2)$$

where \hat{H}_{el} represents the electronic Hamiltonian operator. The 1^1A_1 , 2^1A_1 , and 1^1B_1 states cannot interact in first order via out-of-plane modes for symmetry reasons. The definition of a diabatic electronic representation that differs from the adiabatic picture is therefore not required within this three-dimensional electronic subspace for a simulation of the dynamics of out-of-plane vibrations. Section III will show that nuclear motion along several normal coordinates of a_2 and b_2 symmetry can induce significant CI with higher lying states, but no unitary transformations of adiabatic electronic state vectors to minimize nonadiabatic couplings are performed in the present study. The $\gamma_{kl}^{(n)}$ coefficients compiled in Table 1 are consequently defined with respect to an adiabatic electronic basis.

Technically, the on-diagonal $\gamma_{kk}^{(n)}$ coefficients are obtained from a fit to the (5,5) CASSCF potential energies of the 1^1A_1 , 2^1A_1 , and 1^1B_1 states as a function of the Q_k for displacements Δ_k from 0.0 to 0.4, while the off-diagonal parameters $\gamma_{kl}^{(n)}$ are calculated using the formula

$$\gamma_{kl}^{(n)} = \frac{V_n(Q_k = \Delta_k, Q_l = \Delta_l) - V_n(Q_k = \Delta_k, Q_l = -\Delta_l)}{4\Delta_k\Delta_l} \quad (k \neq l) \quad (2.3)$$

Dimensionless normal coordinate displacements $\Delta_k = \Delta_l = 0.1$ from the equilibrium geometry have been employed to determine the $\gamma_{kl}^{(n)}$ constants.

Approximate normal frequencies for the out-of-plane vibrations in the 1^1A_1 , 2^1A_1 , and 1^1B_1 states can then be obtained from the Hessian matrices γ by first calculating the matrix $\hat{\omega}^2$ for each state according to²⁷

$$\hat{\omega}^2 = \omega^{1/2}(2\gamma)\omega^{1/2} \quad (2.4)$$

Here, ω denotes the diagonal matrix of harmonic ground-state frequencies. The elements of ω must be the frequencies of the normal modes in terms of which the γ matrices are defined. Diagonalization of $\hat{\omega}^2$ and taking the square root of the diagonal elements yields approximate normal frequencies $\hat{\omega}_k$ in the respective electronic state.

III. Results and Discussion

The resulting Hessian matrices for the 1^1A_1 , 2^1A_1 , and 1^1B_1 states of CHT (Table 1) indicate pronounced differences between ground and excited state force fields for the out-of-plane modes. The absolute values of the off-diagonal coefficients $\gamma_{kl}^{(n)}$ do not exceed 0.0032 eV in the 1^1A_1 state, providing evidence that the MP2 and CASSCF S_0 normal coordinates are nearly parallel, but some large normal coordinate rotations are calculated for excitation into the 2^1A_1 and 1^1B_1 vibronic manifolds. For the transition $1^1A_1 \rightarrow 2^1A_1$, Duschinsky mixing⁸ is particularly strong between the pairs Q_{14}/Q_{19} , Q_{15}/Q_{17} , Q_{18}/Q_{19} , Q_{32}/Q_{35} , whereas considerable coupling of the pairs Q_{17}/Q_{18} , Q_{18}/Q_{19} and Q_{33}/Q_{34} is predicted upon $1^1A_1 \rightarrow 1^1B_1$ excitation.

For the calculation of approximate normal frequencies in the 1^1A_1 , 2^1A_1 , and 1^1B_1 states according to eq 2.4, the MP2/aug-cc-pVDZ ground-state frequencies are employed to construct the diagonal matrix ω because the $\gamma_{kl}^{(n)}$ coefficients are defined with respect to the corresponding normal coordinates. The resulting frequencies for the out-of-plane vibrations in the 1^1A_1 , 2^1A_1 , and 1^1B_1 states can be found in Table 2. A comparison of the (5,5) CASSCF ground state frequencies with experiment reveals generally good agreement, except for the CH₂ wagging distortions ν_{16} and ν_{33} , which are underestimated by more than 60 cm⁻¹.

Massive excited-state frequency shifts are calculated for several out-of-plane displacements at the (5,5) CASSCF level of theory. The topology of the 2^1A_1 and 1^1B_1 potential energy functions can differ so considerably from the shape of the oscillators in the 1^1A_1 state that an unambiguous correlation of ground state normal vibrations with excited state modes is not possible in all cases. In other words, large off-diagonal $\gamma_{kl}^{(n)}$ parameters in the excited state Hessian matrices lead to eigenvectors of $\hat{\omega}^2$ that are not dominated by a single basis vector but represent linear combinations with significant contributions from two or more basis vectors. Some of the distortions along the ground state normal coordinates of a_2 and b_2 symmetry illustrated in Figures 1 and 2, respectively, are therefore substantially modified in the excited states. The a_2 normal modes ν_{18}/ν_{19} and the b_2 displacements ν_{32}/ν_{35} resemble symmetric/antisymmetric linear combinations of the corresponding ground-state eigenvectors in the 2^1A_1 state, for example.

Experimental information about frequencies in the 2^1A_1 state is available from $hv + hv$ REMPI,^{7,8} one-photon fluorescence

b_2 Modes

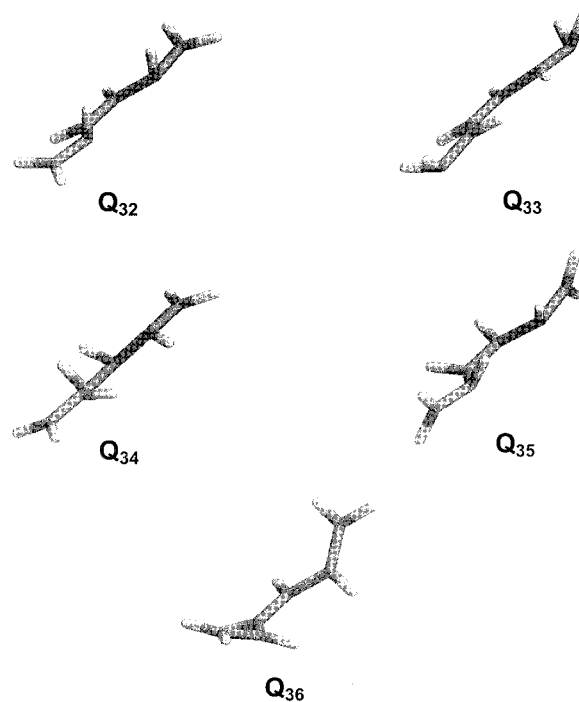


Figure 2. Displacements along the five b_2 symmetry ground-state normal coordinates of cis-1,3,5-hexatriene are shown. The geometries can be described by the C_s point group.

TABLE 2. Approximate Harmonic Vibrational Frequencies of the Out-of-Plane Modes of cis-1,3,5-hexatriene in the 1^1A_1 , 2^1A_1 and 1^1B_1 States Obtained at the (5,5) CASSCF/aug-cc-pVDZ Level of Theory by Employing Formula eq 2.4. For the 1^1A_1 State, the Calculated Values Are Compared to Observed Fundamental (anharmonic) Frequencies^a

symmetry	mode	1^1A_1 (experiment)	1^1A_1 (theory)	2^1A_1 (theory)	1^1B_1 (theory)
a_2	ν_{14}	1032 [44]	1028.6	822.2	1005.4
	ν_{15}	952 [44]	947.6	681.0	910.6
	ν_{16}	907 [44]	841.4	377.0	822.9
	ν_{17}	714 [6]	693.2	-202.3	484.8
	ν_{18}	330 [5]	324.2	274.2	235.9
	ν_{19}	160 [45]	163.5	90.8	-181.1
b_2	ν_{32}	990 [45]	1050.7	854.7	1027.0
	ν_{33}	910 [46]	843.0	354.4	856.1
	ν_{34}	825 [45]	809.0	685.0	775.2
	ν_{35}	589 [46]	602.1	-146.5	472.4
	ν_{36}	110 [45]	109.5	153.1	100.0

^a Units are in cm⁻¹

excitation,⁹ and RR spectroscopy⁴ in the gas phase, but the assignment of out-of-plane modes has not been attempted in the experimental papers^{4,7-9} and clearly requires theoretical support. The CASSCF studies by Kohler et al.⁸ and Olivucci et al.,¹⁷ already mentioned in section II, lead to the conclusion that the CH₂ wagging motions ν_{16} and ν_{33} ⁸ and the methylene torsions ν_{17} and ν_{35} ¹⁷ could have drastically reduced frequencies in the 2^1A_1 state. Our calculations essentially confirm these predictions for all four modes and will be shown to comply with the experimental observations.

Figure 3 reproduces the low-frequency region of the free jet $hv + hv$ REMPI spectrum of the 2^1A_1 state of CHT reported by Kohler et al.⁸ The lowest energy feature in the 2^1A_1 REMPI spectrum appears as a doublet with a splitting of ~ 5 cm⁻¹ and

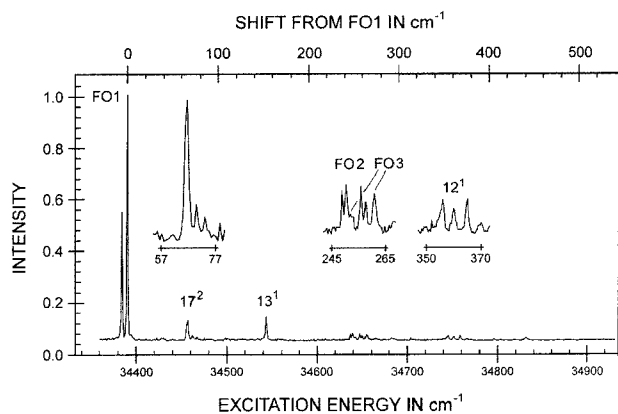


Figure 3. The $1^1A_1 \rightarrow 2^1A_1$ transition of cis-1,3,5-hexatriene: low-frequency region of the experimental $h\nu + h\nu$ REMPI excitation spectrum (in supersonic jet expansion) (Ref 8) with tentative assignment of prominent peaks.

has been shown to be a false origin (FO1) built on one quantum of the b_1 symmetry mode ν_{31} ,^{1,2,4,29} blueshifted by 210–280 cm^{-1} with respect to the 0–0 level of the 2^1A_1 oscillator.^{2,29}

The idea that the second transition of the FO1 doublet could represent the fundamental or the first overtone of a very low frequency mode with a vibrational excitation energy of 5 cm^{-1} appears very unlikely because an extended progression in this vibration would have been expected.⁸ The nonplanarity of CHT in the electronic ground state and the possibility that the lowest energy component of FO1 corresponds to a hot band have been ruled out as explanations for the appearance of FO1 as a doublet in Ref 8. The option that tunneling splitting of level ν_{31}^1 could be induced by a single out-of-plane displacement characterized by a shallow double minimum potential energy function in the excited state can also be excluded because the upper of the two out-of-plane components would be nontotally symmetric and the level thus vibrationally forbidden. On the basis of their own CASSCF calculations, Kohler et al. postulate that the doublet structure may be due to two nearly degenerate minima on the S_1 potential energy surface corresponding to distortions along Q_{16} and Q_{33} .⁸ The out-of-plane frequencies compiled in Table 2 suggest, however, that displacements along Q_{17} and Q_{35} may in reality be responsible for the splitting of FO1. This scenario is also consistent with the doublet appearance of two bands at $\sim 253 \text{ cm}^{-1}$ and $\sim 258 \text{ cm}^{-1}$ above FO1 (see below) and with the 5 cm^{-1} splitting of a very weak feature located 280 cm^{-1} below FO1 that has tentatively been assigned as the 0–0 transition of the 2^1A_1 state in Ref 29.

The next strong band in the 2^1A_1 REMPI spectrum is located 67 cm^{-1} above the vibronic origin FO1 and represents a triplet with a prominent first peak (Figure 3). This group of levels probably corresponds to excitations based on FO1² and most likely reflects quadratic Franck–Condon activity in one or several out-of-plane modes because no totally symmetric mode is expected to have such a low fundamental frequency in the 2^1A_1 state. One possible candidate is the activation of methylene torsions. Inspection of Table 1 suggests an identification of the transition at 67 cm^{-1} with the overtone ν_{17}^2 because of the large reduction of the diagonal coupling coefficient $\gamma_{kk}^{(n)}$ by nearly 70% for this mode in the 2^1A_1 state as compared to the ground state, leading to a considerable Franck–Condon factor for this level. However, a prediction of the energy of the ν_{17}^2 transition based on the Hessian matrix cannot be made due to the imaginary frequency of this mode.

The main intensity of the 67 cm^{-1} band probably does not arise from excitation of level ν_{35}^2 because the $\gamma_{kk}^{(n)}$ value in the 2^1A_1 state is reduced by only 30% relative to the ground state for this mode. We therefore infer that the Franck–Condon factors for a transition into level ν_{35}^2 is smaller than for ν_{17}^2 . An identification of the feature at 67 cm^{-1} exclusively with level ν_{17}^2 leads to the question of why this signal appears as a triplet. Kohler and co-workers⁸ speculate that the multiplet patterns observed for this and several other transitions in the low-energy region of the REMPI spectrum could be induced by a lifting of the degeneracy of torsional levels associated with two shallow double minimum potentials in the 2^1A_1 state via barrier tunneling. However, if the assignment of the band at 67 cm^{-1} to level ν_{17}^2 is correct, then only ν_{35} could modulate this transition according to Table 2. This, however, would lead to a doublet structure with a much weaker or completely dark upper component for symmetry reasons.

The alternative view, that the multiplet structure of level ν_{17}^2 arises from a rotation of CHT around the C_2 axis,² will be examined next. This argument is supported by the similarity of the rotational profiles of FO1²⁹ and of the vibronic origin band of the 2^1A_g state of all-trans-octatetraene³⁰ to the band at 67 cm^{-1} in the 2^1A_1 REMPI spectrum of CHT. Both molecules rotate around the C_2 axis upon excitation of the false origins, a rotational orientation consistent with an alignment of the transition dipole moment parallel to the π -bond axis due to intensity borrowing from the S_2 state. Free jet one-photon fluorescence excitation spectroscopy of the 2^1A_1 state of CHT reveals the rotational P and R branches of the three lowest lying vibronic levels⁹ and a contour analysis of the partially rotationally resolved FO1 doublet confirms the identification as a parallel band.²⁹ A comparison with the rotational envelopes of the false origins of CHT and octatetraene suggests an identification of the triplet ranging from 62 to 77 cm^{-1} with the partially resolved R branch, whereas the much weaker feature between 57 and 62 cm^{-1} may represent the P branch of this rovibronic band. This interpretation implies that the rotational resolution in the REMPI spectrum is $>2 \text{ cm}^{-1}$ as compared to the $<1 \text{ cm}^{-1}$ spacing of the rotational transitions associated with the vibronic origins of CHT and octatetraene evident from the fluorescence excitation spectra in Refs 29 and 30.

Not only were the rotational resolution in the REMPI spectrum lower, it is striking that the band at 67 cm^{-1} would appear as the only vibronic transition with a pronounced rotational structure as can be seen from Figure 3. The combination of two properties may contribute to a selective enhancement of rotational features of this particular level: (i) A lifetime $\tau_1(E)$ of $>5 \text{ ps}$ and (ii) the fact that an out-of-plane vibration is excited. $\tau_1(E)$ has been estimated to lie between 5 ps and 15 ns on resonance with the first band in the 2^1A_1 REMPI spectrum, then decreases to 2.5 ps at 770 cm^{-1} above FO1 and reaches an asymptotic value of $\sim 730 \text{ fs}$ beyond 4000 cm^{-1} excess vibrational energy.^{31–33}

The strong dependence of $\tau_1(E)$ on the excitation energy can be inferred from a comparison of the intensity ratios of corresponding signals in REMPI and fluorescence excitation spectra. The intensity ratio is close to one for the transition at 67 cm^{-1} but drops to 0.45 and 0.2 for the bands at 152 cm^{-1} and 245–265 cm^{-1} , respectively.⁹ The reduction of $\tau_1(E)$ with increasing excess vibrational energy obviously quenches the fluorescence emission more effectively than the REMPI ionization yield. However, a possible lifetime- and consequently energy-dependent rotational resolution in the REMPI spectrum

cannot explain the absence of a rotational structure for FO1. It can only be speculated that activation of the methylene torsions may lead to an increased sensitivity of the REMPI method to rotational features, but a mechanism to support this hypothesis cannot be provided at present.

Finally, we discuss the idea that the triplet at 67 cm^{-1} may correspond to a group of two or three nearly degenerate vibronic bands. This option may seem unlikely considering the regular, equidistantly spaced level structure but cannot be disproved based on the available data. The strong first transition must then again be assigned as the first overtone of ν_{17} if this version is accepted, whereas at least one of the much weaker satellites at $\sim 71\text{ cm}^{-1}$ and $\sim 75\text{ cm}^{-1}$ may result from excitation of the level ν_{35}^2 (see Table 2).

The band at 152 cm^{-1} above FO1 is again built on level ν_{31}^1 and can be attributed to the fundamental of the totally symmetric vibration ν_{13} , whereas the complex feature ranging from 245 to 265 cm^{-1} probably corresponds to two vibronic transitions, a doublet centered at $\sim 253\text{ cm}^{-1}$ and characterized by a width of $\sim 7\text{ cm}^{-1}$ with an additional splitting of each peak by $\sim 1\text{ cm}^{-1}$ and another doublet with components located at $\sim 253\text{ cm}^{-1}$ and $\sim 262\text{ cm}^{-1}$. One of the doublets can be tentatively identified as a second false origin level, ν_{30}^1 or FO2, with an excess vibrational energy of $475\text{--}545\text{ cm}^{-1}$ relative to the true or electronic origin of the 2^1A_1 state.² The second doublet will be assigned to another false origin, FO3, induced by second-order $2^1A_1\text{--}1^1B_1$ coupling via modes ν_{16} and ν_{36} . An excess vibrational energy of $\sim 530\text{ cm}^{-1}$ is projected for this combination level in Table 2. The splittings of FO1, FO2, and FO3 are therefore of similar magnitude, and in particular for FO1 and FO3 also the intensity ratios, suggesting that all three transitions are modulated by the same out-of-plane modes. The origin of the additional splitting of FO2 by $\sim 1\text{ cm}^{-1}$ is not clear. Table 7 in Ref 1 predicts a $2^1A_1\text{--}1^1B_1$ coupling activity for ν_{31} that is 3.4 times higher than that of ν_{30} , but the ratio of the integrated REMPI intensities of FO1 and FO2 + FO3 is 13:1.⁸ The low intensity of FO2 + FO3 is likely a consequence of the dependence of the photoionization yield on $\tau_1(E)$.

A group of three nearly equidistantly spaced peaks ranging from 350 to 370 cm^{-1} above FO1 represents another contribution to the intensity distribution in the low-frequency region of the 2^1A_1 REMPI spectrum shown in Figure 3. All three levels are built on FO1 because no mode of b_1 symmetry or combination of modes of a_2 and b_2 symmetries of appropriate frequencies is present to promote a fourth false origin in this energy domain and no significant vibronic activity based on FO2/FO3 is expected at these excess vibrational energies. We propose here the identification of this triplet with level ν_{12}^1 assuming that the frequency of ν_{12} in the excited state is reduced by $\sim 30\text{ cm}^{-1}$ with respect to the electronic ground state. The linear Franck–Condon activity in the totally symmetric mode ν_{12} in the 2^1A_1 state has been predicted to exceed that of ν_{13} so that the fundamental of ν_{12} is expected to appear in the REMPI spectrum.¹ The observation that the transition ν_{12}^1 appears with the same integrated intensity in the REMPI spectrum than ν_{13}^1 ⁸ despite a greater coupling strength of ν_{12} in the 2^1A_1 state as compared to ν_{13} can again be explained by the dependence of the REMPI intensities on $\tau_1(E)$. Modulation by out-of-plane vibrations is likely responsible for the appearance of level ν_{12}^1 as a triplet.

Kohler et al. note the absence of multiplet features analogous to those observed for CHT in the REMPI spectra of the S_1 states of alkyl substituted hexatrienes. Alkyl substitution can lead to a significant modification of the potential energy functions for

out-of-plane modes and to a quenching of level splittings evident in the spectra of the unsubstituted CHT molecule.

To conclude our considerations of out-of-plane activity in the 2^1A_1 state of CHT, we will analyze the origin of the massive frequency shifts. The decrease of frequencies of a_2 modes can be related to the coupling of the 2^1A_1 state with states of 1A_2 symmetry because the direct product of the irreducible representations of these vibrations and of the electronic states contains the totally symmetric representation

$$A_1 \otimes a_2 \otimes A_2 \supset A_1 \quad (3.1)$$

Possible coupling partners are the $1^1A_2(3p\sigma)$, $2^1A_2(3d\delta)$, and $3^1A_2(3s)$ Rydberg states³ with experimentally determined vertical excitation energies of 6.08 eV ,^{35–38} 6.51 eV ,^{35–39} and 7.40 eV ,³⁹ respectively. Vibronic interactions of compact valence states with diffuse Rydberg states are generally not very strong, but $\langle y^2 \rangle$ expectation values (y being the coordinate perpendicular to the molecular plane) close to $50 a_0^2$ have been obtained at the CASSCF level of theory for all three 1A_2 states in Ref 3. The 1A_2 Rydberg states are consequently predicted to be relatively localized so that vibronic coupling with the 2^1A_1 state ($\langle y^2 \rangle = 33.8 a_0^2$ ³) may in fact be pronounced along certain displacements of a_2 symmetry.

Modes that transform according to the symmetry species b_2 of the C_{2v} point group can stabilize the 2^1A_1 state via interaction with the proximate $1^1B_2(3s)$, $2^1B_2(3p\sigma)$, $3^1B_2(3d\delta)$, and $4^1B_2(3d\sigma)$ Rydberg states³ (experimental vertical excitation energies: 5.66 eV ,³⁵ 5.88 eV ,³⁹ 6.60 eV ,³⁹ and 6.79 eV ,³⁹ respectively) because

$$A_1 \otimes b_2 \otimes b_2 \supset A_1 \quad (3.2)$$

The $\langle y^2 \rangle$ expectation values of CASSCF wave functions of the first three states of 1B_2 symmetry are also close to $50 a_0^2$ ³ and, therefore, quite compact for Rydberg excitations, a result that supports the idea of significant valence-Rydberg interaction through selected modes of b_2 symmetry. The mode with the lowest frequency in the ground state, in this case ν_{36} , represents an exception as the single out-of-plane vibration with a positive frequency shift in the 2^1A_1 state. Normal coordinate rotations cannot be invoked to account for this effect. An argument based on bond order reorganization following the electronic transition is complicated by the fact that a frequency increase and decrease is calculated for the single-bond torsions ν_{36} and ν_{19} , respectively, in the 2^1A_1 state. A comparison of the distortions Q_{19} and Q_{36} (see Figures 1 and 2) suggests that electronic repulsion effects are critical for the excited-state frequencies of both modes.

Ascribing the frequency shifts in the 2^1A_1 state to vibronic interactions with higher lying configurations thus represents not the only possible way to analyze the computational results. An alternative interpretation can be given that attempts to rationalize the frequency changes in terms of electronic structure differences between ground and excited state. The $1^1A_1 \rightarrow 2^1A_1$ transition leads to modifications of the rotational constants for CHT that are consistent with a significant bond order reversal upon excitation.²⁹ For example, in this picture, the dramatically reduced frequencies of methylene torsions in the 2^1A_1 state can be explained by a substantial weakening of the terminal double bonds present in ground-state CHT.

The differentiation between intrastate and interstate effects as origins of the excited-state frequency shifts is a semantic one, of course, because this classification depends on the perspective of the viewer, in the same way that diabatic and

adiabatic electronic representations are different descriptions of the same physical situation. The idea of an “isolated” 2^1A_1 state clearly can only serve as an abstract model because vibronic interactions with other electronic states have to be considered in the calculation of the potential energy functions.

Information about the normal frequencies of the 1^1B_1 state is available from absorption¹⁰ and RR spectroscopy^{5,6} as well as from electronic structure calculations.^{11,18,19} From a fit to the gas-phase absorption envelope of the 1^1B_1 state based on vapor phase RR spectra, Amstrup et al.⁵ and Ci and Myers⁶ estimate the fundamental frequencies of several modes of a_1 , a_2 , and b_2 symmetry in the 1^1B_1 state. Ref 6 reports identical frequencies in ground and excited states for ν_{14} , ν_{15} , and ν_{17} . For ν_{14} and ν_{15} , this is in agreement with Table 2 and the calculations in Refs 11 and 18. However, theory predicts a frequency reduction for ν_{17} by 13%⁵ to 30% (Ref 18 and Table 2). The following frequency shifts in the 1^1B_1 state have been obtained from RR scattering for other out-of-plane vibrations: for ν_{18} , from -12% ⁵ to -25% ,⁶ for ν_{19} , from -51% ⁵ to $+15\%$,⁶ and for ν_{35} , -27% .⁵ From electronic structure theory, moderate to considerable excited-state frequency reductions are predicted for the torsional modes ν_{18} , ν_{19} , and ν_{35} by the CIS,^{18,19} CASSCF¹⁹ and PPP models.¹¹ The different sources thus agree that the out-of-plane frequencies are generally lower in the 1^1B_1 state than in the 1^1A_1 state, a result also confirmed by the present study (Table 2). Although Amstrup et al.⁵ assume a 1^1B_1 potential surface that is bound with respect to all twisting coordinates, a stabilizing effect of the C–C single bonds and methylene torsions on the 1^1B_1 state has been predicted by Ci and Myers.⁶ From this point of view, the imaginary frequency for ν_{19} given in Table 2 is consistent with Ref 6, despite the moderate frequency increase postulated for ν_{19} by Ci and Myers. Ab initio calculations by Zerbetto and Zgierski also indicate that the 1^1B_1 energy is stabilized by Q_{19} .¹⁸

It has been noted in section II that out-of-plane Hessian matrices are generally not expected to vary significantly with totally symmetric coordinates if the displacements are small. The dependence of the potential energy on normal coordinate Q_{18} appears to change strongly in the 1^1B_1 state, however, if evaluated at the substantially different minima of the 1^1A_1 and 1^1B_1 states. CIS and CASSCF calculations carried out by Rohlfing indicate that the optimized C_{2v} structure of the 1^1B_1 state could be unstable with respect to a distortion along Q_{18} , contrary to Refs 11 and 18. The equilibrium geometry of the diabatically correlated 1^1B state is proposed to correspond to a configuration of C_2 symmetry that is twisted by 90° around the central C=C bond in Ref 19 (see also Ref 40). It is obviously important in this case to differentiate where in coordinate space the Hessian matrix for the 1^1B_1 state is evaluated. The intensities of transitions in the RR and absorption spectra of the 1^1B_1 state reflect the excited-state Hessian matrix at the equilibrium geometry of the electronic ground state. The assumption of an imaginary frequency for mode ν_{18} at the minimum of the 1^1B_1 state is therefore absolutely consistent with the results of gas-phase RR spectroscopy^{5,6} and the calculations performed for this work.

An analysis of Duschinsky mixing upon $1^1A_1 \rightarrow 1^1B_1$ excitation can be found in the semiempirical study by Hemley et al.¹¹ and in the RR investigation by Amstrup et al.⁵ Ref 11 only considers totally symmetric modes and predicts strong normal coordinate rotations between ν_8 and ν_9 and between ν_9 and ν_{10} . The considerable mixing of ν_8 and ν_9 is also confirmed by a simulation of the 1^1B_1 RR excitation profiles in Ref 2.

The Duschinsky mixing between ν_{18} and ν_{19} inferred by Amstrup et al. is large but not as pronounced as suggested by Table 1.

Vibronic interaction of the 1^1B_1 state with the nearby 1^1B_2 Rydberg states represents an obvious mechanism for the reduced 1^1B_1 frequencies of a_2 modes in the vapor phase

$$B_1 \otimes a_2 \otimes B_2 \supset A_1 \quad (3.3)$$

By analogy, a strong frequency reduction of ν_{35} in the 1^1B_1 state can be interpreted as being due to the coupling of the 1^1B_1 state with the adjacent 1^1A_2 Rydberg states

$$B_1 \otimes b_2 \otimes A_2 \supset A_1 \quad (3.4)$$

The 1^1B_1 valence state ($\langle y^2 \rangle = 41.0 a_0^2$ at the CASSCF level of theory;³ this value will shrink if dynamical electron correlation is included) is less compact than the 2^1A_1 state so that significant interaction with moderately diffuse Rydberg states can be expected.

RR measurements of CHT in solution carried out by Ci and Myers further demonstrate that the gas-phase frequency shifts for a_2 modes in the 1^1B_1 state are systematically reduced in polarizable media. This means that the ground and excited-state force constants converge with increasing polarizability of the solvent,⁶ while the energy for the $1^1A_1 \rightarrow 1^1B_1$ transition decreases. The origin band for excitation into the ionic 1^1B_1 state (calculated dipole moment $+0.421 \text{ au}^{3,41}$) is red shifted by -2367 cm^{-1} in cyclohexane at room temperature,⁶ for example. By contrast, the covalent 2^1A_1 state (calculated dipole moment $-0.097 \text{ au}^{3,41}$) is known to be relatively insensitive to solvent effects,⁴² which leads to a significant decrease of the vertical $2^1A_1 - 1^1B_1$ energy difference in polarizable solvents, enhancing the vibronic coupling between the two states.⁶ A parallel increase of the energy separating the 1^1B_1 and 1^1B_2 states could provide a mechanism for the intensity quenching upon solvation observed in the 1^1B_1 RR spectra for bands involving vibrations of a_2 symmetry. Unfortunately, no measurements of solvent shift effects on 1^1B_2 Rydberg states are available. The dipole moments of -2.026 au and $+2.172 \text{ au}$ calculated for the 1^1B_2 and 2^1B_2 Rydberg states, respectively, are large, but the wave functions are also more diffuse than that of the 1^1B_1 valence state,^{3,41} so that it is difficult to predict the magnitude of stabilization of the 1^1B_2 and 2^1B_2 states in polarizable media without an extensive simulation. An analogous frequency increase in the condensed phase may be the reason for the suppression of RR activity in the a_u modes recorded for the 1^1B_u state of THT, induced by a hypothetical enlargement of the $1^1B_u - 1^1B_g$ energy difference in polarizable liquids.⁴³ It might, therefore, prove worthwhile to model solvent shift effects on the RR spectroscopy of CHT and THT using, for example, molecular mechanics techniques.

In summary, the (5,5) CASSCF model appears to yield Hessian matrices for the 2^1A_1 and 1^1B_1 potential energies as a function of the out-of-plane coordinates that agree satisfactorily with the spectroscopic observations of both excited states. It is clear that a higher-order description of the out-of-plane potential energy functions is required to fully resolve the individual contributions of vibrations, barrier tunneling and possibly also rotations to the intriguing multiplet patterns in the low-frequency region of the REMPI spectrum of the 2^1A_1 state. The Duschinsky mixing of out-of-plane modes in the excited states is of great importance for an understanding of the intensity distributions in RR and excitation spectra of the 2^1A_1 and 1^1B_1 states. An attempt to include dynamic electron correlation into the

electronic structure model via the CASPT2 method based on (5,5) CASSCF reference functions was not successful. An extension of the active space would probably be required but is presently not feasible. The discussion in this section has shown that CI in particular with low-lying Rydberg configurations induces significant frequency shifts of out-of-plane modes in the 2^1A_1 and 1^1B_1 states. The option to consider these strong couplings more accurately by treating the interacting states in a balanced way appears to be interesting but imposes serious difficulties from an electronic structure perspective.

Acknowledgment. We gratefully acknowledge support from the National Science Foundation under Grant No. CHE-9727562. The authors would also like to thank Professor Wybren J. Buma (University of Amsterdam), Professor Wolfgang Domcke (Technical University of Munich), and Professor Joseph I. Cline (University of Nevada, Reno) for stimulating discussions and Jeremy Murray (University of Nevada, Reno) for his help in preparing the figures for this work.

References and Notes

- (1) Woywod, C.; Livingood, W. C.; Frederick, J. H. *J. Chem. Phys.* **2001**, *114*, 1631.
- (2) Woywod, C.; Livingood, W. C.; Frederick, J. H. *J. Chem. Phys.* **2001**, *114*, 1645.
- (3) Serrano-Andrés, L.; Roos, B. O.; Merchán, M. *Theor. Chim. Acta* **1994**, *87*, 387.
- (4) Westerfield, C.; Myers, A. B. *Chem. Phys. Lett.* **1993**, *202*, 409.
- (5) Amstrup, B.; Langkilde, F. W.; Bajdor, K.; Wilbrandt, R. *J. Phys. Chem.* **1992**, *96*, 4794.
- (6) Ci, X.; Myers, A. B. *J. Chem. Phys.* **1992**, *96*, 6433.
- (7) Buma, W. J.; Kohler, B. E.; Song, K. *J. Chem. Phys.* **1990**, *92*, 4622.
- (8) Buma, W. J.; Kohler, B. E.; Song, K. *J. Chem. Phys.* **1991**, *94*, 6367.
- (9) Petek, H.; Bell, A. J.; Christensen, R. L.; Yoshihara, K. *J. Chem. Phys.* **1992**, *96*, 2412.
- (10) Leopold, D. G.; Pendley, R. D.; Roebber, J. L.; Hemley, R. J.; Vaida, V. *J. Chem. Phys.* **1984**, *81*, 4218.
- (11) Hemley, R. J.; Lasaga, A. C.; Vaida, V.; Karplus, M. *J. Phys. Chem.* **1988**, *92*, 945.
- (12) Lengsfeld III, B. H.; Yarkony, D. R. *Adv. Chem. Phys.* **1992**, *82*, 1.
- (13) Roos, B. O. *Adv. Chem. Phys.* **1987**, *69*, 399.
- (14) Roos, B. O.; Taylor, P. R.; Siegbahn, P. E. M. *Chem. Phys.* **1980**, *48*, 157.
- (15) Werner, H.-J. *Adv. Chem. Phys.* **1987**, *69*, 1.
- (16) Ruedenberg, K.; Schmidt, M. W.; Gilbert, M. M.; Elbert, S. T. *Chem. Phys.* **1982**, *71*, 41.
- (17) Olivucci, M.; Bernardi, F.; Celani, P.; Ragazos, I.; Robb, M. A. *J. Am. Chem. Soc.* **1994**, *116*, 1077.
- (18) Zerbetto, F.; Zgierski, M. Z. *J. Chem. Phys.* **1993**, *98*, 4822.
- (19) Rohlfing, C. (private communication).
- (20) H. Petek, A. J. Bell, Y. S. Choi, K. Yoshihara, B. A. Tounge, and R. L. Christensen *J. Chem. Phys.* **1993**, *98*, 3777.
- (21) Buma, W. J.; Zerbetto, F. *J. Am. Chem. Soc.* **1996**, *118*, 9178.
- (22) Woon, D. E.; Dunning, T. H., Jr. *J. Chem. Phys.* **1993**, *98*, 1358.
- (23) Cave, R. J.; Davidson, E. R. *J. Phys. Chem.* **1988**, *92*, 614.
- (24) Cave, R. J.; Davidson, E. R. *Chem. Phys. Lett.* **1988**, *148*, 190.
- (25) Andersson, K.; Blomberg, M. R. A.; Fülscher, M. P.; Karlström, G.; Lindh, R.; Malmqvist, P.-Å.; Neogrády, P.; Olsen, J.; Roos, B. O.; Sadlej, A. J.; Schütz, M.; Seijo, L.; Serrano-Andrés, L.; Siegbahn, P. E. M.; Widmark, P. O. { t MOLCAS, Version 4.0; Lund University: Sweden, 1997.
- (26) Andersson, K.; Roos, B. O. *Int. J. Quantum Chem.* **1993**, *45*, 591.
- (27) Cederbaum, L. S.; Domcke, W. *Adv. Chem. Phys.* **1977**, *36*, 205.
- (28) Duschinsky, F. *Acta Physicochim. (USSR)* **1937**, *7*, 551.
- (29) Rijkensberg, R. A.; Bebelar, D.; Buma, W. J. *J. Am. Chem. Soc.* **2000**, *122*, 7418.
- (30) Petek, H.; Bell, A. J.; Choi, Y. S.; Yoshihara, K.; Tounge, B. A.; Christensen, R. L. *J. Chem. Phys.* **1995**, *102*, 4726.
- (31) Fuss, W.; Schikarski, T.; Schmid, W. E.; Trushin, S. A.; Hering, P.; Kompa, K. L. *J. Chem. Phys.* **1997**, *106*, 2205.
- (32) Cyr, D. R.; Hayden, C. C. *J. Chem. Phys.* **1996**, *104*, 771.
- (33) Cyr, D. R.; Hayden, C. C. In *Laser Techniques for State-Selected and State-to-State Chemistry III*; Hepburn, J. W., Ed.; Proc. SPIE **1995**, *2548*, 103.
- (34) Buma, W. J.; Kohler, B. E.; Song, K. *J. Chem. Phys.* **1991**, *94*, 4691.
- (35) Sabljic, A.; McDiarmid, R. *J. Chem. Phys.* **1986**, *84*, 2062.
- (36) Gavin, R. M., Jr.; Risemberg, S.; Rice, S. A. *J. Chem. Phys.* **1973**, *58*, 3160.
- (37) Gavin, R. M.; Rice, S. A. *J. Chem. Phys.* **1974**, *60*, 3231.
- (38) Flicker, W. M.; Mosher, O. A.; Kuppermann, A. *Chem. Phys. Lett.* **1977**, *45*, 492.
- (39) Doering, J. P.; Sabljic, A.; McDiarmid, R. *J. Phys. Chem.* **1984**, *88*, 835.
- (40) Nebot-Gil, I.; Malrieu, J.-P. *J. Chem. Phys.* **1982**, *77*, 2475.
- (41) Usually, only the magnitude of the dipole moment vector is reported, but Ref 3 gives, in addition, the sign. The orientation of the vector along the C_2 axis is unfortunately not clear from Ref 3.
- (42) Hudson, B. S.; Kohler, B. E.; Schulten, K. In *Excited States*; Lim, E. C., Ed.; Academic: New York, 1982; Vol. 6, p 1.
- (43) Woywod, C.; Livingood, W. C.; Frederick, J. H. *J. Chem. Phys.* **2000**, *112*, 613.
- (44) Langkilde, F. W.; Wilbrandt, R.; Nielsen, O. F.; Christensen, D. H.; Nicolaisen, F. M. *Spectrochim. Acta* **1987**, *43A*, 1209.
- (45) McDiarmid, R.; Sabljic, A. *J. Phys. Chem.* **1987**, *91*, 276.
- (46) Lippincott, E. R.; Kenney, T. E. *J. Am. Chem. Soc.* **1962**, *84*, 3641.